Available online at www.sciencedirect.com
SCIENCE DIRECT
Polymer 47 (2006) 1778–1784
polymer
www.elsevier.com/locate/polymer

Polypyrrole micro- and nanowires synthesized by electrochemical polymerization of pyrrole in the aqueous solutions of pyrenesulfonic acid

Gewu Lu, Chun Li, Gaoquan Shi *

Department of Chemistry and Lab of Bio-Organic Phosphorus, Tsinghua University, Beijing 100084, People's Republic of China

Received 21 November 2005; received in revised form 22 January 2006; accepted 24 January 2006

Abstract

Polypyrrole (PPy) micro- and nanowires were synthesized through electrochemical polymerization of pyrrole in the aqueous solutions of 1-pyrenesulfonic acid (PSA), in which PSA acted as both surfactant and dopant. Macroscopic studies (SEM and TEM) indicated that the PPy wires have diameters of 120–500 nm and length of several micrometers. Electrochemical investigation demonstrated that the PPy wires have much stronger electrochemical activity than the conventional flat PPy film because of their higher specific surface area. Furthermore, the PSA doped PPy wires showed strong emission in an aqueous dispersion. A possible micelle guided formation mechanism has been proposed and investigated.

Keywords: Polypyrrole; 1-Pyrenesulfonic acid; Electrochemical polymerization

1. Introduction

The design and construction of conducting polymer-based macro- or nanostructures have become a topic of increasing interest due to their potential applications in electrical, optical and sensing devices [1–6]. Several intriguing approaches have been explored for fabricating these novel structures, such as chemical or electrochemical polymerization within nanoporous templates [7–11], surfactant-mediated synthesis [12–17], 'soap-bubble' template synthesis [18–20], interfacial polymerization [21], seeding polymerization [22], electrospinning [23], mechanical stretching [24] and catalytic polymerization [25]. Moreover, it is also well known that various conducting polymers can self-assemble into nanostructures both in solutions [26,27] and at the interfaces [28]. Of these methods, surfactant-mediated synthesis is one of the attractive and convenient means of obtaining nanostructured conducting polymers because surfactant has versatile and remarkable self-assembly ability and can form various novel nanostructures.

Pyrene and its derivatives have unique fluorescence properties, which can be used as a fluorescent-probe for the detection of DNA base radicals, an indicator for bio-gas sensor, and a press-sensitive material [29,30]. In the present work, our attention has been focused on the creation of nanostructured conducting polymers doped with an amphiphilic pyrene derivative, 1-pyrenesulfonic acid (PSA), and thus the obtained composites will combine the properties of low-dimensional material, conducting polymers, and the functional pyrene dopant. Herein, we report the electrochemical synthesis of polypyrrole (PPy) in the aqueous solutions of PSA. In this medium PSA acted as both surfactant and electrolyte. The influences of electrochemical polymerization conditions such as total charge density used for polymerization and concentrations of PSA on the morphology of PPy micro- and nanowires were investigated.

2. Experimental

Pyrrole (Chinese Army Medical Institute, Beijing, China) was purified by distillation under nitrogen atmosphere before use. 1-Pyrenesulfonic acid (PSA) was purchased from Aldrich and used without further purification. De-ionized water was used throughout this work.

The electrochemical polymerization and examinations were performed in a one-compartment cell with the use of a potentiostat-galvanostat (Model 283, EG&G Princeton Applied Research) under computer control. A stainless steel sheet (SS, AISI 304, $5\times10\ mm^2$) was used as the working electrode and a Pt sheet ($18\times10\ mm^2$) was applied as the counter electrode. These two electrodes were placed 1 cm apart. SS was carefully polished with abrasive paper (1200 mesh), cleaned with water and acetone successively

* Corresponding author. Tel.: +86 10 6277 3743; fax: +86 10 6277 1149.
E-mail address: gshi@tsinghua.edu.cn (G. Shi).

0032-3861/$ - see front matter © 2006 Elsevier Ltd. All rights reserved.
doi:10.1016/j.polymer.2006.01.081

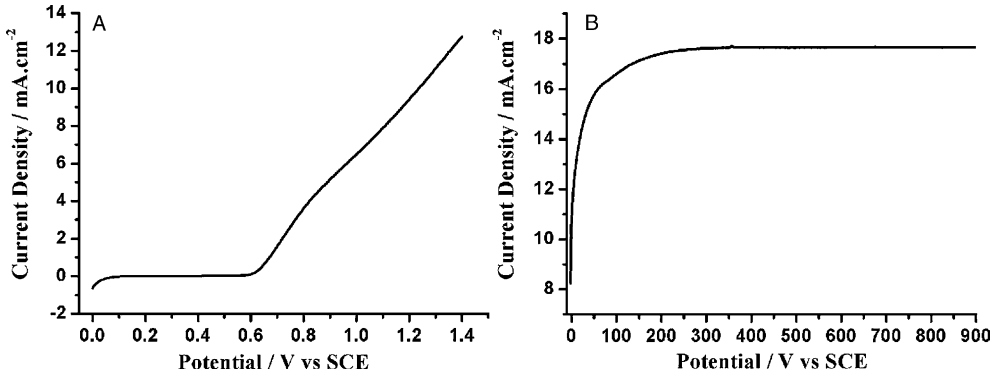

Fig. 1. (A) Anodic polarization curve of 16.7 mM pyrrole in the aqueous solution of 35 mM PSA at a potential scan rate of 50 mV s^{-1}; (B) chronoamperogram for the oxidation of 16.7 mM pyrrole at 1.1 V in the aqueous solution of 35 mM PSA.

and dried before each experiment. All potentials were referred to a saturated calomel electrode (SCE). The typical electrolyte was 30 ml H_2O contained 0.34 ml pyrrole (≈16.7 mM) and 0.04–0.42 g PSA (≈4.7–50 mM). All solutions were deaerated by bubbling dry nitrogen gas and maintained under a slight overpressure during the experiments. The PPy films were grown potentiostatically at 1.1 V (vs. SCE) and their thickness was controlled by the total charges passed through the cell which were read directly from the *I–t* curves by computer. After polymerization, the films were washed repeatedly with water to remove the electrolyte and monomer. The same instruments were used for the voltammetry measurements. For the studies of luminescence, the obtained samples were first immersed in 2 M NaOH for one day and successively dipped in water for 2 days, then filterated and rinsed with water for several times and dried in vacuum. All the experiments were carried out at room temperature.

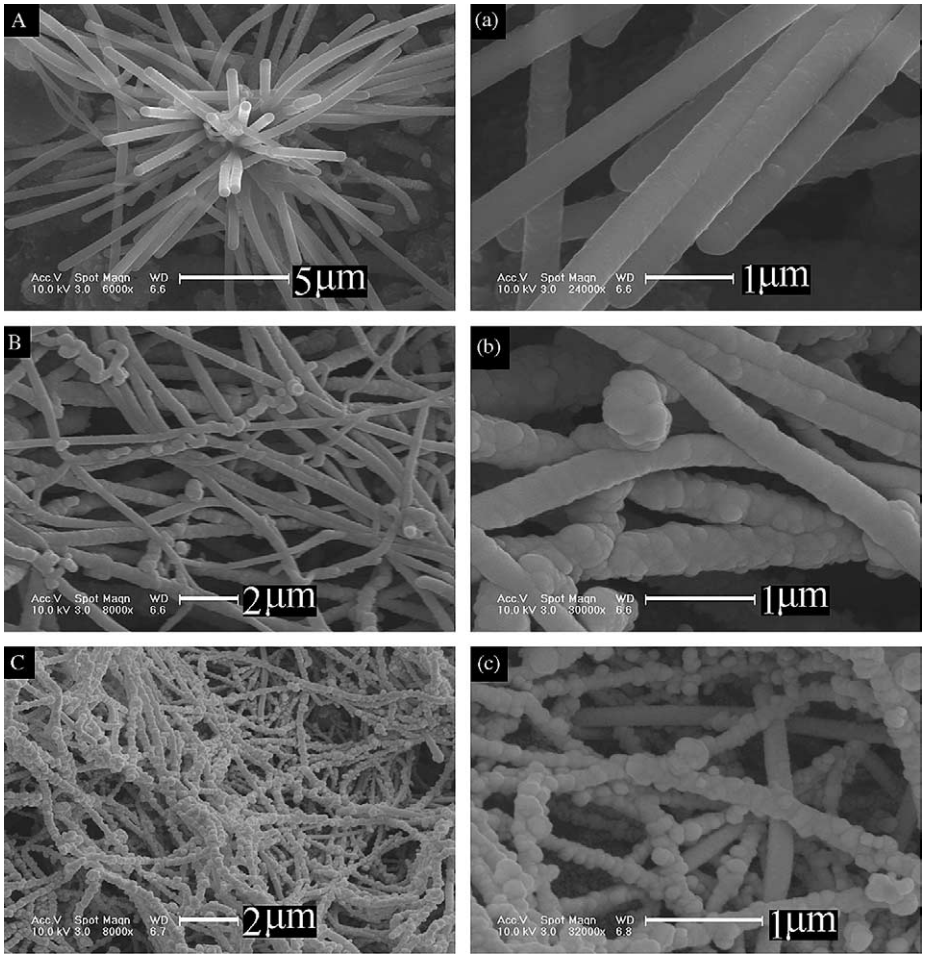

Fig. 2. SEM images of the PPy structures synthesized by electrochemical oxidation of 16.7 mM pyrrole at 1.1 V for 3.94 C cm^{-2} each in the electrolytes with different PSA concentrations: (A) 25 mM, (B) 35 mM, (C) 50 mM; a, b, c, are the magnified images corresponding to A, B, C, respectively.

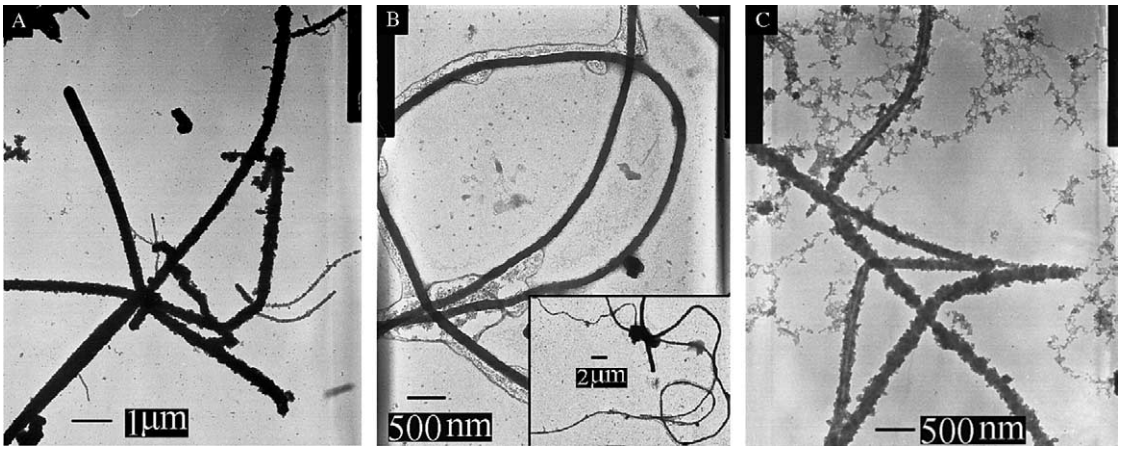

Fig. 3. TEM images of the PPy nanostructures synthesized by electrochemical oxidation of 16.7 mM pyrrole at 1.1 V for 3.94 C cm^{-2} each in the electrolytes with different PSA concentrations: (A) 25 mM, (B) 35 mM, (C) 50 mM. Inset of Fig. B is the full image corresponding to (B).

Raman spectra were recorded by using a microscopic confocal Raman spectrometer using a 785-nm laser beam and a charge-coupled detector (CCD) with 4 cm^{-1} resolution. The spectra were recorded by using a 50× objective and the laser power was always kept very low (0.1 mW) to avoid destruction of the samples. For the Raman measurements, the samples were first ultrasonicated in water, and then dropped the dispersions on a clean glass by burette and dried before experiments. Scanning electron micrographs were taken out using a KYKY 2800 electron micrographer (Scientific Instrument of Chinese Academy, China) and the transmission electron micrographs were obtained using a JEM2010 electron microscope (JEOL, Japan). Fluorescence spectra were carried out on a Perkin–Elmer LS 55 luminescence spectrometer. The ionic conductivity of the PSA aqueous solution was measured at room temperature by using a DDS-307 conductivity gauge (Shanghai Rex Instrument Factory, Shanghai, China).

3. Results and discussion

Polypyrrole wires can be electrochemically grown on various substrates such as stainless-steel (SS), indium tin oxide glass (ITO) and platinum. To produce the wires economically on large electrode surface, stainless steel electrode was selected in this study. Fig. 1(A) shows the anodic polarization curve of pyrrole at SS in the aqueous solution of 35 mM PSA. This figure exhibits that the virgin

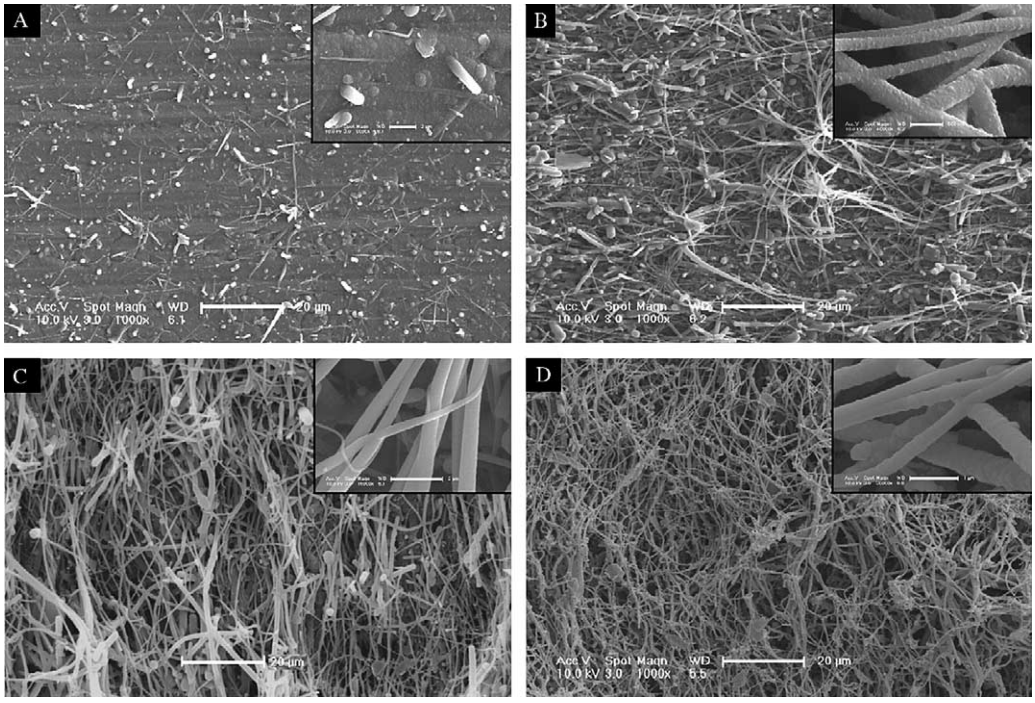

Fig. 4. SEM images of the PPy wires synthesized potentiostatically in the aqueous solution of 35 mM PSA at 1.1 V for a charge density of: (A) 0.198 C cm^{-2} (20 s), (B) 1.261 C cm^{-2} (120 s), (C) 2.356 C cm^{-2} (240 s), and (D) 3.524 C cm^{-2} (400 s). Bar scale, 20 μm; inset bar scale, 1 μm.

oxidation of pyrrole is initiated at approximately 0.70 V (vs. SCE). The strong anodic current wall led to the formation of PPy. The current transition curve for the oxidation of pyrrole at 1.1 V is presented in Fig. 1(B). During the polymerization process, pyrrole monomers were oxidized into radical cathions and then coupled into soluble oligomers. When a critical degree of polymerization was reached, or when the concentration of the oligomers exceeded their solubility limit, PPy was deposited on the surface of working electrode [31–33]. This process was associated with a rise in measured current as shown in the initial stage of Fig. 1(B) [34]. After a transitory period (about 180 s), a stationary growth regime was reached, showing that the deposited morphology remained globally invariant.

The SEM images the PPy wires deposited on SS electrodes are shown in Fig. 2. As can be seen from figures, the concentration of PSA (C_{PSA}) affects strongly on the morphology of the wires. As C_{PSA} was lower than 25 mM, the resulting products composed mainly particles and only a few wires located sparsely on the electrode surface (Fig. S1, Supporting Information). When C_{PSA} was increased up to 25 mM, smooth PPy wires with average diameter of ca. 400 nm and length of 1–10 μm were densely generated and aggregated into dendritic structures (Fig. 2(A) and (a)). With the increase of PSA concentration, the diameters of the wires decreased, while the surfaces of the wires became rough gradually (Fig. 2(A)–(C)). The optimal concentration of PSA for growing homogeneous small sized PPy wires with smooth surfaces in a large scale was tested to be around 35 mM (Fig. 2(B) and (b)).

The formation of the fibrous PPy structures was also confirmed by the TEM images (Fig. 3). Because the SEM pictures were taken out after a vapor deposition of about 20 nm gold layer on the PPy wires, while the samples used for TEM detection was in naked state. Therefore, there is a little diameter difference between the wires shown in corresponding SEM and TEM images. It is also clear from this figure that the wires can reach as long as several micrometers. Furthermore, the wires are curved and entangled, demonstrating they are flexible (inset of Fig. 3(B)).

The PPy wires were possibly formed through micelle guided growth process. In general, surfactant exists in the electrolyte as molecules or micelles depending strongly on its concentration. The structures of the micelles may change from spherical to rod- and lamellar-shape as the concentration of the surfactant was increased, which influenced on the morphology of PPy wires. The properties of the PSA micelle phase have been simply studied by measuring its ionic conductivity (Fig. S2, Supporting Information). The results indicated that spherical micelles were formed in the solution as C_{PSA} was higher than about 5 mM and they undergone structural transition to rod-like micelles as C_{PSA} was increased up to 30 mM. When C_{PSA} was in the region of 5 and 30 mM, large numbers of spherical micelles existed in the electrolyte and could be assembled on to electrode surface under the function of a positive potential [35]. Meanwhile, pyrrole is considered to be preferentially dissolved into the micellar assembly because of the hydrophobic nature of the monomer. Therefore, the micelles adsorbed on the electrode surface acted as the templates and the pyrrole inside the micelles was polymerized mainly into particles (Fig. S1, panes A–D). On the other hand, as the surfactant concentration increased to be over 30 mM, PPy wires were generated as the main product based on the rod-like micelles (Figs. S1 and 2).

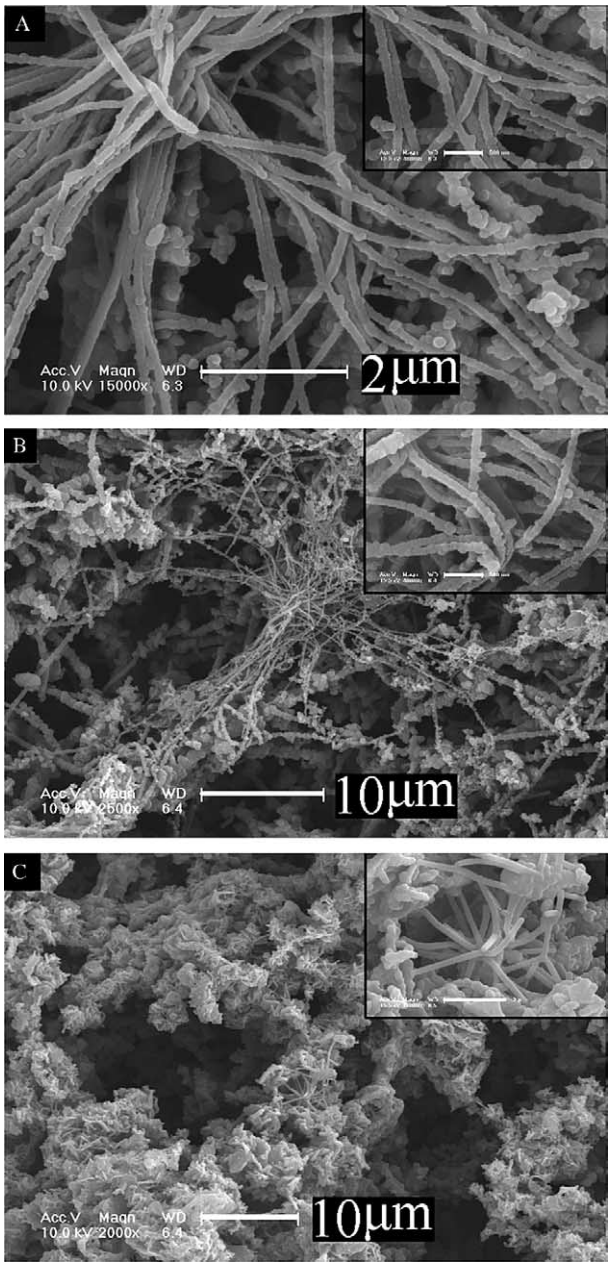

Fig. 5. SEM images of the PPy structures synthesized by electrochemical oxidation of 16.7 mM pyrrole at 1.1 V for 3.94 C cm^{-2} each in the electrolytes with the same PSA concentration (35 mM) and different NaCl concentrations: (A) 28 mM, (B) 42 mM, (C) 80 mM. Inset bar scales: (A, B) 500 nm, (C) 2 μm.

Template and seeding effects of the PSA micelles for the formation of the PPy wires were also confirmed by the SEM images recorded during the electropolymerization process (Fig. 4). At the initial stage of polymerization of pyrrole in 35 mM PSA solution at 1. 1 V (20 s, 0.198 C cm^{-2}), PPy particles and fibrils were nucleated on the whole electrode

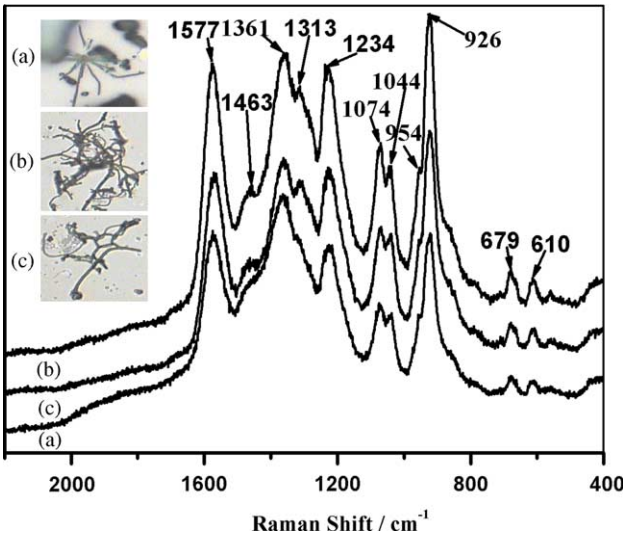

Fig. 6. Raman spectra of the PPy wires synthesized from the media with different PSA concentrations: (a) 25 mM, (b) 35 mM, (c) 50 mM.

surface (pane A). The density of the fibrils increased with electrolysis time and reached maximum within 2 min (pane B, 1.261 C cm^{-2}). After this stage, the fibrils continued to grow in their length (panes A–D). Finally, a network of PPy wires was generated (pane D). Another proof for the dual role of the PSA micelle is that the length of the PPy wires increased but the diameters of the wires maintained almost as a constant with the increase of polymerization time. From the regional magnified image of pane B (inset), it is expected that the grains of the formed wires might act as external nucleation sites for the formation of PPy wires, which facilitate the formation of the network.

In addition, it is known that an inorganic electrolyte can alter the properties of micelles such as their morphology and critical concentration. Therefore, we studied the effect of NaCl on the morphology of the PPy wires and the results are illustrated in Fig. 5. It is clear from this figure that the addition of certain amount of NaCl (20–40 mM) in the electrolyte of 35 mM PSA can reduce the diameters of the wires from about 400 nm (Fig. 2(B) and (b)) to around 100 nm (Fig. 5(A) and (B)). However, if the concentration of NaCl was very high (e.g. 80 mM), the quality of the wires became very poor (Fig. 5(C)). These results strongly support that the wires were formed through a micelle template route.

The Raman and FTIR spectroscopy were used to characterize the structure of the obtained PPy wires. As shown in Fig. 6, the microscopic Raman spectra of the PPy wires synthesized in the media with different PSA concentrations are similar to each other and give the characteristic bands of PPy prepared by the conventional methods [36,37]. The band at 1577 cm^{-1} is assigned to C=C stretching and the skeletal band appears at 1463 cm^{-1}. The bands at 1361 and 1234 cm^{-1} are attributed to the C–N stretching and C–H in plane bending, respectively [36]. The C–H in plane bending and the ring deformation associated with dications are at 1074 and 926 cm^{-1}, while those related to radical cations are at 1044 and 954 cm^{-1} [37]. Therefore, it appears that in each case, both charge carriers contribute to the conductivity of PPy–PSA wires.

The typical FTIR spectra of the PPy wires prepared at different conditions are also identical to each other (Fig. 7(A)). The peak at 1035 cm^{-1} belongs to $-SO_3^-$ group of the dopants [38], indicating that the PPy wires are doped by PSA. The 1537 cm^{-1} peak is assigned to the stretching vibration of the C=C double bond of PPy [39]. The C–N stretching vibration peak of PPy appears at 1457 cm^{-1}. The peaks at 1300 and 1166 cm^{-1} represent the =C–H in-plane vibration [40]. Furthermore, the weak band around 1700 cm^{-1} is attributed to the carbonyl group, which indicates that PPy is slightly overoxidized during the growth process. X-ray diffraction pattern of PPy wires (Fig. 7(B)) exhibits a broad peak at $2\theta = 23.4°$ ($d = 3.79$ Å), which is assigned to the scattering from PPy chain at the interplanar spacing in the PPy–PSA [41,42]. The results imply that the PPy chains in the PPy wires have ordered arrangement to some extent.

The electrochemical properties of PPy films synthesized at different dopant concentration were investigated by cyclic voltammetry at a relatively slow scan rate (Fig. 8). Each CV cycle was stabilized by multiple CV scanning for ionic exchanges. As can be seen from this figure, all the samples are electrochemically active, and each CV shows a couple of strong and broad redox waves. Amongst them, the PPy wires

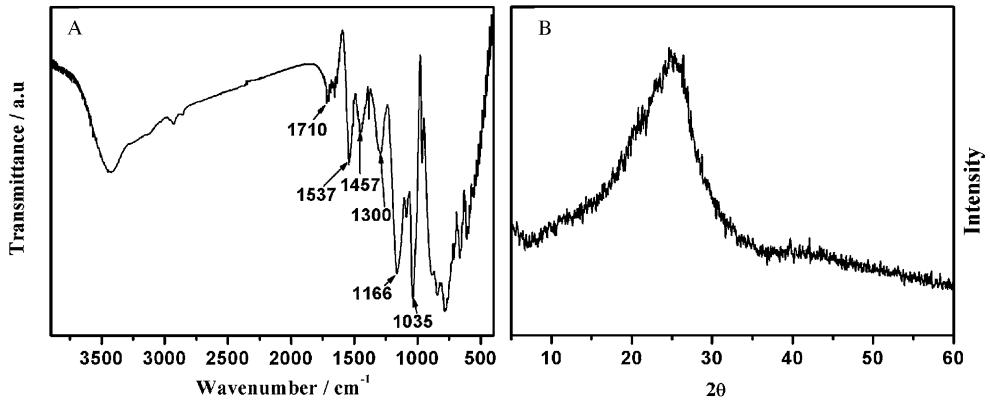

Fig. 7. FTIR spectrum (A) and X-ray diffraction pattern (B) of the typical PPy wires.

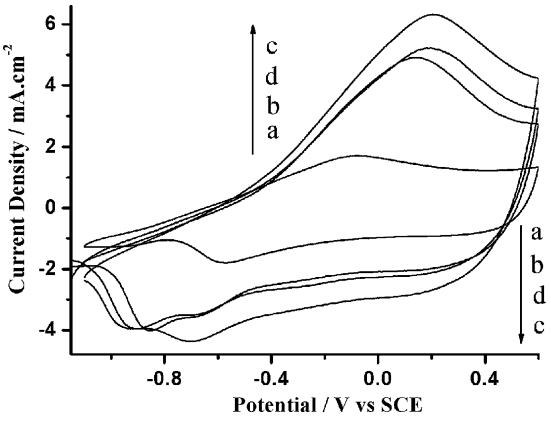

Fig. 8. Cyclic voltammogramms for PPy films in 0.1 M TBATFB acetonitrile solutions at scan rate of 10 mV s^{-1}. PPy films were synthesized by electrolysis for same charge density of 2.5 C cm^{-2} from the media with different PSA concentrations. (a) 4.7 mM, (b) 25 mM, (c) 35 mM (d) 50 mM. All voltammogramms were recorded after 100 CV scans in the same potential range at a scan rate of 50 mV s^{-1}.

prepared from 35 mM aqueous solution of PSA has the highest redox current density, indicating that the networks of PPy wires formed at this condition has the highest specific active surface area. It is noted here that the voltammograms show two reduction peaks, attributing to a dual mode of anion and cation exchange, a characteristic of the PPy film with a large anionic dopant [43].

The excitation and emission spectra of aqueous PSA solution, PPy wires dispersed in water and the filtrate of PPy dispersion are illustrated in Fig. 9. All the emission spectra exhibit two peaks at 377 and 397 nm and a shoulder at 416 nm as the samples were excited at 346 nm (the excitation spectra show strong bands at 331 and 346 nm), which is in good agreement with the results reported previously [44–46]. However, the emission intensity of aqueous PPy nanowire dispersion is about three times that of its filtrate. Considering the fact that the samples of PPy wires were carefully washed (Section 2) to remove PSA that may adsorb on the wire surface, the emission of PPy wire is mostly resulted from the PSA incorporated into PPy matrix, which gives a further evidence

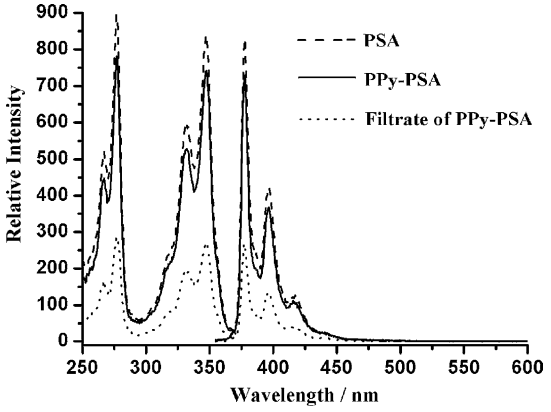

Fig. 9. Excitation and emission spectra of 5×10^{-5} M PSA aqueous solution, PPy wires dispersed in water (1.5 mg PPy in 200 ml water) and the corresponding filtrate.

that the PPy wires were doped by PSA. While the emission of the filtrate of PPy wires might be due to the release of PSA from the PPy matrix by ultrasonication.

4. Conclusions

PPy micro- and nanowires with the diameter of 120–500 nm and the length of several micrometers can be readily fabricated in a large scale through electrochemical polymerization of pyrrole in the presence of PSA on various electrodes. The concentration of PSA is a key factor for the formation of PPy micro- and nanowires. The obtained PPy wires have higher electrochemical activity in comparison with the films, which make them become an attractive candidate for the construction of sensing devices. It is worth noting that all the PSA doped PPy wires show strong emission in aqueous dispersion, which provides potential applications in fabrication of various optoelectric devices.

Acknowledgements

This work was supported by National Natural Science Foundation of China (20374034, 50225311, 90401011, 50533030) and 973 Project (2003CB615700).

Supplementary data

Supplementary data associated with this article can be found, in the online version, at doi:10.1016/j.polymer.2006.01.081

References

[1] MacDiarmid AG. Angew Chem. Int Ed 2001;40(14):2581–90.
[2] Wallace GG, Innis PC. J Nanosci Nanotechnol 2002;2(5):441–51.
[3] Lu GW, Chen F, Wu XF, Qu LT, Zhang JX, Shi GQ. Chin Sci Bull 2005;50(16):1673–82.
[4] Malinauskas A. Polymer 2001;42(9):3957–72.
[5] Malinauskas A, Malinauskiene J, Ramanavicius A. Nanotechnology 2005;16(10):R51–R62.
[6] Bay L, West K, Skaarup S. Polymer 2002;43(12):3527–32.
[7] Martin CR. Acc Chem Res 1995;28(2):61–8.
[8] Jérôme C, Demoustier-Champagne, Legras R, Jérôme R. Chem Eur J 2000;6(17):3089–93.
[9] Fu MX, Zhu YF, Tan RQ, Shi GQ. Adv Mater 2001;13(24):1874–7.
[10] Qu LT, Shi GQ. Chem Commun 2004;(24):2800–1.
[11] Dauginet-Da Pra L, Demoustier-Champagne S. Polymer 2005;46(5):1583–94.
[12] Goren M, Qi ZG, Lennox RB. Chem Mater 2000;12(5):1222–8.
[13] Wei ZX, Zhang ZM, Wan MX. Langmuir 2002;18(3):917–21.
[14] Huang K, Wan MX. Chem Mater 2002;14(8):3486–92.
[15] Wei ZX, Wan MX. Adv Mater 2002;14(18):1314–7.
[16] He C, Yang CH, Li YF. Synth Met 2003;139:539–45.
[17] Wu AM, Kolla H, Manohar SK. Macromolecules 2005;38(19):7873–5.
[18] Qu LT, Shi GQ, Chen FE, Zhang JX. Macromolecules 2003;36(4):1063–7.
[19] Yuan JY, Qu LT, Shi GQ. Chem Commun 2004;(8):994–5.
[20] Bajpai V, He PG, Dai LM. Adv Funct Mater 2004;14(2):145–51.
[21] Huang JX, Kaner RB. J Am Chem Soc 2004;126(3):851–5.
[22] Zhang XY, Manohar SK. J Am Chem Soc 2004;126(40):12714–5.

[23] MacDiarmid AG, Jones WE, Norris ID, Gao J, Johnson AT, Pinto NJ, et al. Synth Met 2001;119(1–3):27–30.
[24] He HX, Li CZ, Tao NJ. Appl Phys Lett 2001;78(6):811–3.
[25] Lee HT, Liu YC. Polymer 2005;46(24):10727–32.
[26] Li C, Hatano T, Masayuki T, Shinkai S. Chem Commun 2004;(20): 2350–1.
[27] Li C, Numata M, Bae AH, Sakurai K, Shinkai S. J Am Chem Soc 2005; 127(13):4548–9.
[28] Guo L, Wu ZK, Liang YQ. Chem Commun 2004;(14):1664–5.
[29] Huber R, Fiebig T, Wagenknecht HA. Chem Commun 2003;(15):1878–9.
[30] Basu BJ, Anandan C, Rajam KS. Sens Actuators B-Chem 2003;94(3): 257–66.
[31] Higgins SJ, Hammett A. Electrochim Acta 1991;36(14):2123–34.
[32] Fermin DJ, Scharifker BR. J Electroanal Chem 1993;357(1/2):273–87.
[33] Scharifker BR, Fermin DJ. J Electroanal Chem 1994;365(1/2):35–9.
[34] Belamie E, Argoul F, Winter R. J Electrochem Soc 2001;148(4): C301–C9.
[35] Naoi K, Oura Y, Maeda M, Nakamura S. J Electrochem Soc 1995;142(2): 417–22.
[36] Han GY, Shi GQ. Sens Actuators B-Chem 2004;99(2,3):525–31.
[37] Duchet J, Legras R, Demoustier-Champagne S. Synth Met 1998;98(2): 113–22.
[38] Varela H, Bruno RL, Torresi RM. Polymer 2003;44(18):5369–79.
[39] Kim JW, Liu F, Choi HJ, Hong SH, Joo J. Polymer 2003;44(1):289–93.
[40] Yang XM, Lu Y. Polymer 2005;46(14):5324–8.
[41] Wynne KJ, Bryan-Street B. Macromolecules 1985;18(12):2361–8.
[42] Ou-Yang JY, Li YF. Polymer 1997;38(15):3997–9.
[43] Bay L, Mogensen N, Skaarup S, Sommer-Larsen P, Jorgensen M, West K. Macromolecules 2002;35(25):9345–51.
[44] Tachikawa T, Ramaraj R, Fujitsuka M, Majima T. J Phys Chem B 2005; 109(8):3381–6.
[45] Grätzel M, Kalyanasundaram K, Thomas JK. J Am Chem Soc 1974; 96(26):7869–74.
[46] Matsumoto H, Koyama Y, Tanioka A. Langmuir 2002;18(9):3698–703.